Inverse Raman scattering in silicon: A free-carrier enhanced effect

D. R. Solli, P. Koonath, and B. Jalali
Department of Electrical Engineering, University of California, Los Angeles, California 90095, USA
(Received 30 October 2008; published 28 May 2009)

Stimulated Raman scattering has been harnessed to produce the first silicon lasers and amplifiers. The Raman effect can also produce intensity-dependent nonlinear loss through a corollary process, inverse Raman scattering (IRS). This process has never been observed in a semiconductor. We demonstrate IRS in silicon—a process that is substantially modified by optically generated free carriers—achieving attenuation levels >15 dB with a pump intensity of 4 GW/cm^2. Surprisingly, free-carrier absorption, the detrimental effect that generally suppresses nonlinear effects in silicon, actually facilitates IRS by delaying the onset of contamination from coherent anti-Stokes Raman scattering. Silicon-based IRS could be a valuable tool for chip-scale signal processing.

DOI: 10.1103/PhysRevA.79.053853 PACS number(s): 42.65.Dr, 42.65.Wi, 42.70.Nq

Raman scattering is an inelastic process that is extremely useful for spectroscopic analysis and can also be used to produce optical gain in a wide variety of transparent media. In its spontaneous form, intense pump light is injected into an optical medium and a minute amount is scattered to redshifted (Stokes) wavelengths by material vibrations. When the process is stimulated by radiation at the Stokes wavelength, it becomes much stronger, as the Stokes wave experiences amplification. As such, stimulated Raman scattering (SRS) has been instrumental in producing silicon-based lasers and amplifiers [1–4]. The Raman effect also couples the pump and Stokes waves with blueshifted (anti-Stokes) waves through a process known as coherent anti-Stokes Raman scattering (CARS). Under the proper conditions, a significant amount of anti-Stokes light is produced [5], which is useful for wavelength conversion [6].

The Raman effect can also produce optical loss through inverse Raman scattering (IRS) [7,8]. In this nonlinear process, light at the anti-Stokes wavelength is attenuated in the presence of an intense pump, opposite to the exponential Stokes gain in Raman amplification. IRS was first reported by Jones and Stoicheff [7] in organic liquids and has been used as a technique for Raman spectroscopy [9]. Since IRS occurs at the anti-Stokes wavelength, it avoids fluorescence contamination [7,9].

Apart from its utility in spectroscopic measurement, IRS could prove to be a valuable tool for photonic signal processing. However, to the best of our knowledge, IRS has never been observed in a semiconductor medium. In this work, we demonstrate the resonant attenuation of an optical signal in a silicon waveguide through IRS. In agreement with the known Raman characteristics of silicon [10], the observed attenuation bandwidth is ~ 100 GHz, but in contrast to SRS, it is blueshifted by 15.6 THz from the pump wavelength. Our numerical simulations indicate that optically generated free carriers actually enhance the level of IRS.

In spontaneous Raman scattering, a minute amount of Stokes light and an even smaller amount of anti-Stokes light are spontaneously radiated, with the proportion determined by the thermal occupation factor of the excited vibrational state. When Stokes or anti-Stokes input waves are added, however, the situation is dramatically different: an input Stokes wave is amplified through SRS, while an input anti-Stokes wave suffers attenuation through IRS (cf. Fig. 1). SRS and IRS are corollary processes, with similar spectral characteristics. Amplification of the Stokes field comes at the expense of pump, whereas, photons are transferred to the pump during the attenuation of the anti-Stokes field.

On the other hand, CARS power transfer between Stokes and anti-Stokes waves depends on the phase mismatch between the pump (k_P), Stokes (k_S), and anti-Stokes (k_{aS}) propagation constants: $\Delta k = 2k_P - k_S - k_{aS}$. Thus, CARS can impact the attenuation suffered by an anti-Stokes signal through IRS. Even in the presence of phase mismatch, significant transfer of energy to the anti-Stokes wave can occur for high pump intensity [11]. The transfer can be reduced by eliminating Stokes input light; however, at high pump power, four-wave mixing coupled with Raman amplification can still produce substantial Stokes radiation, affecting the anti-Stokes attenuation as discussed further below.

In silicon, the landscape is complicated by additional nonlinear effects. In the presence of intense fields, two-photon absorption (TPA) produces broadband attenuation, and generates free carriers, which cause free-carrier absorption (FCA) [12]; these effects result in a self-limiting process that depletes the pump intensity [13]. Simultaneously, self-phase modulation (SPM), produced by a concerted action of the Kerr nonlinearity and free-carrier refraction (FCR), blueshifts the pump spectrum [13]. As the lifetime of free carriers is $\sim 1-10$ ns in silicon waveguides, carrier buildup may be minimized using short pulses with repetition period much longer than the carrier lifetime. Although FCA generally de-

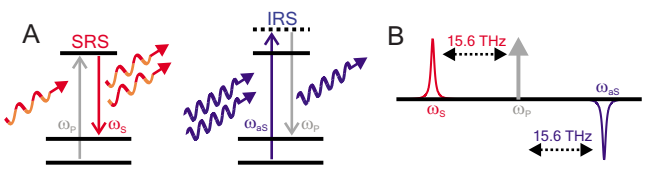

FIG. 1. (Color online) IRS and SRS are corollary processes arising in Raman scattering. (a) SRS: Stokes photons amplified at expense of pump. IRS: anti-Stokes photons absorbed, transferring energy to pump. (b) Raman scattering is a resonant process: redshifted SRS gain line and blueshifted IRS absorption line straddle the pump, spaced by 15.6 THz in silicon.

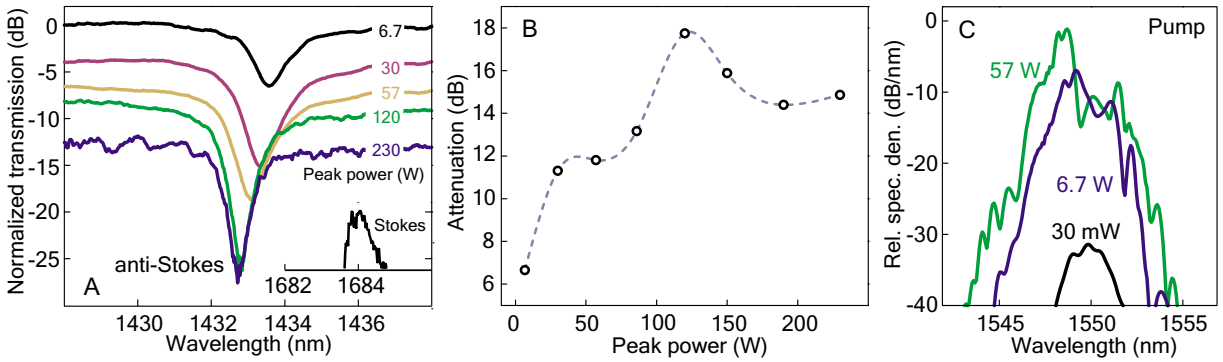

FIG. 2. (Color online) Experimental observation of IRS in silicon. (a) Normalized transmission vs wavelength at indicated pump power levels. IRS causes resonant nonlinear attenuation; broadband loss arises from TPA and FCA. Inset shows transmitted Stokes signal (same y axis from main plot applies). (b) Maximum resonant attenuation (broadband absorption not included) of anti-Stokes signal vs pump power. Inset illustrates waveguide geometry. (c) Measured pump spectra at waveguide output. Nonlinearity blueshifts peak of pump spectrum causing blueshift in IRS line as seen in part a.

grades the performance of silicon devices, we demonstrate that it surprisingly facilitates the observation of IRS, a feature that makes IRS in semiconductors distinctly different from that in other media.

In our experiments, picosecond optical pulses from a mode-locked laser (6 MHz rep. rate, 1.5 ps duration, $\lambda=1550$ nm) are split to produce pump and probe pulses. One portion is stretched, amplified, and compressed to generate 20 ps pump pulses with 2 nm bandwidth and peak power up to 230 W. The other portion is amplified and sent through a nonlinear fiber to generate a flat optical continuum at the anti-Stokes wavelength ($\sim$1433 nm). This continuum, much weaker than the pump and shorter in duration, is filtered to a $\sim$30 nm bandwidth to ensure that it does not contain Stokes energy. The pump and anti-Stokes pulses are synchronized, combined in free space, and coupled to a single-mode silicon waveguide (mode area $\sim 2.8\ \mu m^2$) through a microscope objective. The input coupling loss is estimated to be $\sim 6-7$ dB. The waveguide ($L=2$ cm) has a linear propagation loss of ~ 0.5 dB/cm. At the waveguide output, light is collected using a single-mode fiber. As the pulse repetition period is much longer than the carrier lifetime, interpulse carrier buildup is negligible.

Measured IRS spectra are shown in Fig. 2(a). At the highest pump intensity, the signal minimum becomes comparable to the noise floor. Whereas IRS produces resonant attenuation, TPA (pump photon+anti-Stokes photon) and FCA produce broadband nonlinear loss. These spectral characteristics reflect the corresponding response time scales: TPA and FCA involve electronic transitions and respond essentially instantaneously (although FCA requires nanoseconds to subside); IRS, being a Raman effect, responds according to the phonon ring down time, which occurs on a picosecond time scale.

The resonant IRS attenuation (discounting the broadband absorption) increases rapidly with pump power initially, as expected, but levels off and decreases slightly for high power [cf. Fig. 2(b)]. Nevertheless, IRS attenuation values >15 dB are readily observed. At high pump intensities, we observe the generation of Stokes signal [cf. Fig. 2(a), inset]. The generation of this signal arises primarily from Raman amplification of power transferred coherently from the anti-Stokes probe to the Stokes wavelength. This Stokes signal is also transferred back to the anti-Stokes wavelength via CARS, which tends to limit the observable IRS attenuation. This process coupled with the self-limiting nature of the pump power are likely responsible for the high-power reduction in IRS absorption illustrated in Fig. 2(b). These issues are discussed further in the context of our numerical studies presented below. It may also be noted that the IRS spectrum shifts toward shorter wavelengths as the pump intensity is increased, which results from the SPM-induced blueshift of the pump spectral peak [13] [cf. Fig. 2(c)].

We perform numerical simulations of IRS in silicon using the generalized nonlinear Schrödinger equation (NLSE) for the field envelope $A(z,t)$. This method has been successfully applied to model pulsed SRS in silicon waveguides [14–16]. The equation can be formulated as

$$\frac{\partial A(z,t)}{\partial z} + \frac{i\beta_2}{2}\frac{\partial^2 A(z,t)}{\partial t^2} = i\gamma\left(1+\frac{i}{\omega_0}\frac{\partial}{\partial t}\right)A(z,t)\int_{-\infty}^{t} R(t-t')|A(z,t')|dt' + \left[\frac{i\omega_0 n_{\mathrm{FCR}}}{c} - \frac{\alpha_{\mathrm{FCA}}}{2}\right]A(z,t),$$

where ω_0 is the carrier frequency, β_2 accounts for group-velocity dispersion, γ is the nonlinear coefficient, $R(t)$ is the third-order nonlinear response function, α_{FCA} is the FCA coefficient, and n_{FCR} is the free-carrier contribution to the refractive index. The TPA coefficient is included in the imaginary part of the nonlinear coefficient [15]: $\gamma=\omega_0 n_2/cA_{\mathrm{eff}}+i\beta_{\mathrm{TPA}}/2A_{\mathrm{eff}}$, where the Kerr index and TPA coefficient are $n_2=6\times10^{-5}$ cm^2/GW and $\beta_{\mathrm{TPA}}=0.5$ cm/GW [17], and A_{eff} is the waveguide mode area.

The response function $R(t)=(1-f_R)\delta(t)+f_R h(t)$ includes electronic (instantaneous) and vibrational (delayed) nonlinearities, where the weighting factor f_R normalizes the time-integrated response. In the Fourier domain, the delayed portion of the response can be related to the Raman gain

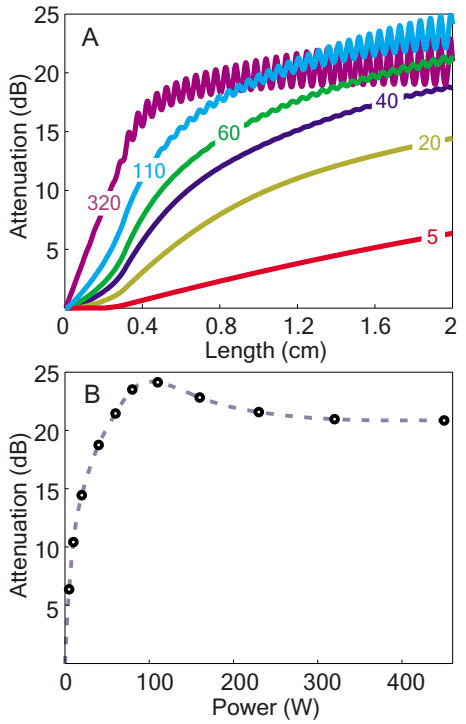

FIG. 3. (Color online) (a) Simulation of IRS attenuation vs propagation length at the indicated pump power levels. At higher power, the attenuation rises rapidly near the start, but levels off further into the waveguide and develops an oscillatory structure due to coherent power transfer. (b) Simulation of IRS attenuation at the waveguide output vs input pump power.

function: $\mathrm{Im}[\tilde{H}(\Omega)]=g(\Omega)/2k_0n_2f_R$, where Ω is the frequency relative to that of the pump ω_P. The gain has frequency dependence: $g(\Omega)\propto\omega/n(\omega)\mathrm{Im}[\chi(\Omega)]$, where $\omega=\Omega+\omega_P$, $n(\omega)$ is the refractive index, and $\chi_R(\Omega)=2\Omega_S\Delta\omega/(\Omega_S^2-\Omega^2-2i\Omega\Delta\omega)$ is the normalized Raman susceptibility. The Raman frequency shift and linewidth are Ω_S and $2\Delta\omega$, respectively. We normalize the gain function to the value $g_R=7$ cm/GW at the Stokes frequency [3,6]. Since $n(\omega_S)\approx n(\omega_{aS})$, we have $\tilde{H}(\Omega)=g_R(\Omega+\omega_P)\chi(\Omega)/[2k_0n_2f_R(-\Omega_S+\omega_P)]$. We assume a Raman linewidth of 105 GHz and a shift of 15.6 THz [10]. When quantifying the IRS attenuation, we smooth the spectrum to reflect a finite spectral measurement resolution of ~1 nm. We start with a chirped pump pulse (20 ps, 2 nm), add a synchronous weak broadband anti-Stokes probe pulse, and monitor the IRS attenuation after transmission through the waveguide ($L=2$ cm, $A_{\mathrm{eff}}=2.8$ μm^2) as in the experiment.

The carrier concentration (produced by TPA) is solved simultaneously with the NLSE using the equation $\partial N_{e=h}(z,t)/\partial t=\beta_{\mathrm{TPA}}|A(z,t)|^4/2\hbar\omega_0A_{\mathrm{eff}}-N_{e=h}(z,t)/\tau$, where τ is the carrier lifetime. As this lifetime is much longer than the pulses, the carrier recombination term can be neglected. The free-carrier refractive-index change and absorption coefficient are found from empirical formulae [18,19]: $n_{\mathrm{FCR}}=-(8.8\times10^{-22}N_e+8.5\times10^{-18}N_h^{0.8})$ and $\alpha_{\mathrm{FCA}}=8.5\times10^{-18}N_e+6.0\times10^{-18}N_h$ (electron, hole densities in cm^{-3} units).

Figure 3(a) shows the calculated anti-Stokes attenuation vs propagation distance. Here, the attenuation increases exponentially initially but levels off with propagation distance. As the pump power is increased, the attenuation develops oscillatory structure and levels off more quickly. For longer propagation lengths, the attenuation increases but ultimately saturates if the pump power is low, but decreases before saturating if the pump power is high. As described above, CARS contamination and the self-limiting nature of the pump limit the IRS attenuation. CARS transfer can limit the IRS attenuation because a significant Stokes signal builds up even when there is no Stokes input. CARS alternates between two processes: generation of Stokes light at the expense of anti-Stokes and generation of anti-Stokes light at the expense of Stokes [5]. Power cycles between Stokes and anti-Stokes wavelengths on a length scale that depends on the phase mismatch: $L=2\pi/\Delta k$. As the phase mismatch here is dominated by material group-velocity dispersion (GVD), we have $L=2\pi/\beta_2\Omega_S^2$. Given silicon's GVD, $\beta_2=1.2$ ps^2/m, we find the oscillation length $L=0.54$ mm, which matches the period in Fig. 3(a). During the cyclical power transfer, the Stokes component is amplified by SRS, which causes Stokes buildup and the resulting CARS contamination effect. As mentioned above, we note that evidence of this mechanism can be identified in the experiment by the observation of a Stokes signal [cf. Fig. 2(b)]. Figure 3(b) shows the anti-Stokes attenuation at the waveguide output as a function of the input pump power. As also seen in the experiment, the attenuation increases to a maximum, but begins to decline at high pump power. These results validate the combined NLSE free-carrier model for IRS in silicon and lend insights into the experimental results.

It is worth noting that the IRS attenuation is generally subject to limitation. If the dispersion is large, the anti-Stokes and Stokes waves are decoupled, which inhibits the CARS contamination of the IRS signal. On the other hand, larger dispersion also causes the pump and anti-Stokes fields to walk off more rapidly limiting the IRS interaction by a different means. For smaller dispersion, the phase mismatch is smaller and CARS contamination takes hold more rapidly. Attempting to increase the pump power enhances the contamination process and also fuels the power-limiting nonlinear absorption of the pump itself. Furthermore, as the anti-Stokes signal is attenuated through IRS, it becomes increasingly vulnerable to CARS contamination because the Stokes wave grows while the anti-Stokes level falls; the transfer of a small fraction of the growing Stokes wave has a substantial impact on the depleted anti-Stokes signal.

Interestingly, the combined NLSE free-carrier model also shows that free-carrier effects actually facilitate the observation of IRS under the present circumstances. Without FCA, the pump power remains larger throughout the waveguide, favoring the growth of the Stokes field and increasing the CARS conversion efficiency. For relatively moderate power levels, CARS contamination becomes so strong that resonant gain is observed at the anti-Stokes wavelength overwhelming the IRS induced attenuation. As a result of pump spectral modifications and dispersion, the CARS and IRS spectra do not overlap perfectly leaving a small amount of residual attenuation (cf. Fig. 4); however, experimentally, this attenua-

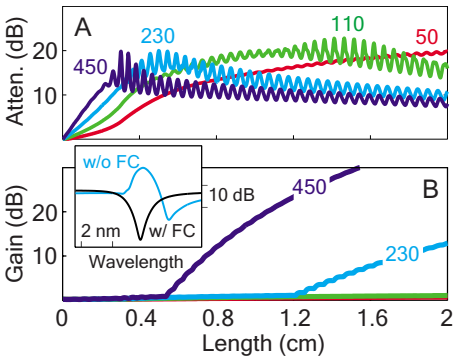

FIG. 4. (Color online) Simulation of the anti-Stokes signal without free carriers. (a) Attenuation from IRS and (b) gain from CARS vs propagation length at the indicated pump power levels. As described, the CARS and IRS spectra do not overlap perfectly, and anti-Stokes gain and attenuation can occur simultaneously. Without carriers, IRS can be masked at the waveguide output. Inset illustrates anti-Stokes spectra with and without free carriers (P=230 W).

tion would be rather difficult to identify *a priori* as the gain becomes the dominant spectral feature. This finding underscores the utility of the model: the influence of free carriers on IRS can be directly assessed. Experimentally, this would be much more difficult to accomplish as reverse-bias carrier sweep-out [2] is not feasible on the time scale of picosecond pulses.

IRS brings another important tool to the silicon photonics toolbox. Chip-scale IRS may have important applications in photonic processing of high-bandwidth radio-frequency signals. For example, it is difficult to perform key mathematical operations and processing functions such as subtraction of two intensity modulated signals because power is fundamentally a positive quantity [20,21]. However, if the Raman pump is intensity modulated at radio frequencies, the IRS signal will have the inverted modulation. With its wavelength flexibility and relatively fast response time of ~3 ps (as determined from its spectral characteristics), IRS is a suitable candidate for performing all-optical switching and modulation functions. As a fast switch, silicon-based IRS may also find application in wavelength-division multiplexing systems, which have been proposed to increase data throughput in optical interconnects.

In summary, we have observed IRS in a semiconductor medium. IRS causes the attenuation of anti-Stokes energy when it propagates with an intense optical pump wave in silicon. Attenuation values in excess of 15 dB have been observed with pump intensities of the order of 4 GW/cm^2. IRS may be very useful for optical signal processing on silicon chips and is an important complementary tool to Raman gain and wavelength conversion via SRS and CARS.

This work was supported by DARPA-MTO.

[1] O. Boyraz and B. Jalali, Opt. Express **12**, 5269 (2004).
[2] H. Rong *et al.*, Nature (London) **433**, 725 (2005).
[3] Q. Xu, V. R. Almeida, and M. Lipson, Opt. Express **12**, 4437 (2004).
[4] V. Raghunathan, O. Boyraz, and B. Jalali, Conference on Lasers and Electro-Optics (CLEO), Baltimore, MD, 2005 (Optical Society of America, Washington, D.C., 2005), Paper number CMU1.
[5] R. W. Boyd, *Nonlinear Optics*, 3rd ed. (Academic Press, New York, 2008).
[6] R. Claps, V. Raghunathan, D. Dimitropoulos, and B. Jalali, Opt. Express **11**, 2862 (2003).
[7] W. J. Jones and B. P. Stoicheff, Phys. Rev. Lett. **13**, 657 (1964).
[8] A. D. Buckingham, J. Chem. Phys. **43**, 25 (1965).
[9] *Non-linear Raman Spectroscopy and Its Chemical Applications*, edited by W. Kiefer and D. A. Long (Bad Winsheim, Germany, 1982).
[10] P. A. Temple and C. E. Hathaway, Phys. Rev. B **7**, 3685 (1973).
[11] P. Koonath, D. R. Solli, and B. Jalali, Conference on Lasers and Electro-Optics (CLEO), Baltimore, MD, 2008 (Optical Society of America, Washington, D.C., 2008), Paper number CThE3.
[12] K. W. DeLong *et al.*, J. Opt. Soc. Am. B **6**, 1306 (1989).
[13] P. Koonath, D. R. Solli, and B. Jalali, Appl. Phys. Lett. **93**, 091114 (2008).
[14] X. Chen, N. C. Panoiu, and R. M. Osgood, IEEE J. Quantum Electron. **42**, 160 (2006).
[15] L. Yin, Q. Lin, and G. P. Agrawal, Opt. Lett. **32**, 391 (2007).
[16] Q. Lin, O. J. Painter, and G. P. Agrawal, Opt. Express **15**, 16604 (2007).
[17] H. K. Tsang *et al.*, Appl. Phys. Lett. **80**, 416 (2002).
[18] R. A. Soref and B. R. Bennett, IEEE J. Quantum Electron. **23**, 123 (1987).
[19] A. Irace *et al.*, *Silicon Photonics*, Topics in Applied Physics, edited by L. Pavesi and D. J. Lockwood (Springer-Verlag, Berlin, 2004), Vol. 94, p. 361.
[20] F. Coppinger *et al.*, IEEE Trans. Microwave Theory Tech. **45**, 1473 (1997).
[21] N. You and R. A. Minasian, J. Lightwave Technol. **22**, 2739 (2004).